LREE	57	**La**	Lanthanum
	58	***Ce***	***Cerium***
	59	**Pr***	Praseodymium
	60	**Nd**	Neodymium
	61	**Pm**	Promethium
lanthanide contraction	62	**Sm**	Samarium
	63	***Eu***	***Europium***
	64	**Gd**	Gadolinium
	65	**Tb***	Terbium
	66	**Dy**	Dysprosium
	67	**Ho***	Holmium
	68	**Er**	Erbium
	69	**Tm***	Thulium
HREE	70	**Yb**	Ytterbium
	71	**Lu**	Lutetium

Simulating the transport and scavenging behavior of rare earth elements in the global ocean.

Yves Plancherel[1], Xinyuan Zheng[1], Samar Khatiwala[1] and Gideon Henderson[1]
[1]Department of Earth Sciences, University of Oxford; yvesp@earth.ox.ac.uk

OCEAN SCIENCES MEETING 2014 - **#17389**
(080) Biogeochemistry of trace elements and their isotopes

UNIVERSITY OF OXFORD — OXFORD MARTIN SCHOOL
NATURAL ENVIRONMENT RESEARCH COUNCIL

Abstract

The oceanic distribution of the rare earth elements (REE), like other insoluble metals (e.g. Th, Pa, Al), represents a balance between sources (rivers and dust), transport and scavenging. As a result of the lanthanide contraction, light REE (LREE) scavenge more readily than heavy REE (HREE) so HREE are more sensitive to transport than LREE resulting in a measureable basin-scale fractionation. Here we use a model, based on the transport matrix formalism, to explore the sensitivity of the REE distribution and the LREE to HREE fractionation to the scavenging intensity associated with multiple particle types (dust, carbonates, silicates, organics), particle sinking velocity, different parameterizations of particle remineralization and various assumptions about source uncertainties. The model solutions are evaluated against a new global compilation of oceanic REE observations using a suite of diagnostics ranging from point-wise comparisons, basin-scale average concentrations, and basin-scale gradients. The results underscore the importance of defining appropriate cost-functions that address possible data coverage artifact (observations are strongly biased towards the Northwest Pacific) in addition to model assumptions when calculating inverse estimates of particulate/dissolved partition coefficients for scavenged-type tracers.

Introduction and rationale

Scavenging (adsorption on marine particles) is an important process that controls the distribution, supply and removal of many elements and isotopes in the ocean. Some metals, however, are not only scavenged but are also bio-utilized (e.g. Fe). The importance of the "abiotic" controls on Fe cycling, for example, is recognized, but poorly known and hard to deconvolve from the complex biological effects. Uncertainties about the role of scavenging, together with the availability of new measurement techniques and an increasing number of data from the GEOTRACES program warrant further investigation on the scavenging process per se.

The lanthanides, or rare earth elements (REEs, atomic numbers between 57 and 71), consist of 14 **economically important elements** (Kato et al. 2011), plus Promethium (Pm, Z=61) which has no stable isotope. The filling of the 4f electron shell with increasing atomic number in the REE sequence induces a progressive reduction of the ionic radius of the REEs (the **lanthanide contraction**), resulting in weak differences in bond strengths when REE interact with other atoms. This produces observable characteristic **fractionation patterns across the REE sequence**. The characteristics of the REE patterns evolves depending on environmental conditions and can be used to study particular geochemical processes.

Dissolved REE in the ocean are present in the +III oxidation state and mostly exist as aqueous complexes (mostly with CO_3^{2-} and the carboxyl groups of organic ligands). It is mostly free ions that adsorb onto particles, however, such that the **particulate-dissolved partitioning**, **source strength** and **sedimentary removal** depend strongly on environmental conditions (pH, pe, pO_2, pCO_2, T, etc.) and on particle types, abundances and fluxes (e.g. Byrne and Shokovitz, 1996; Chase et al. 2002). Since the stability of aqueous complexes for heavy REE (**HREE**) tends to be greater than that for light REE (**LREE**), dissolved REE are relatively enriched in HREE while **particles are enriched in LREE** (Byrne and Sholkovitz, 1996).

Aside from Ce and Eu, which are influenced by redox processes, REEs as a group form a self-consistent sequence of elements that is mainly affected by scavenging in seawater. REEs, in addition to Pa, Th and Be, which have been used traditionally, can thus be used to help understand the relative importance of scavenging and transport processes and further advance our understanding of the main controls of the scavenging process in the ocean.

We report here on results from a suite of global numerical simulations designed to capture the main processes controlling the distribution of REE in seawater. Although numerical models exist for Nd, this is to our knowledge the first global modeling experiment focusing on the REE pattern as a whole that explicitly considers REE sources and REE concentrations.

Global observational coverage and typical REE distributions

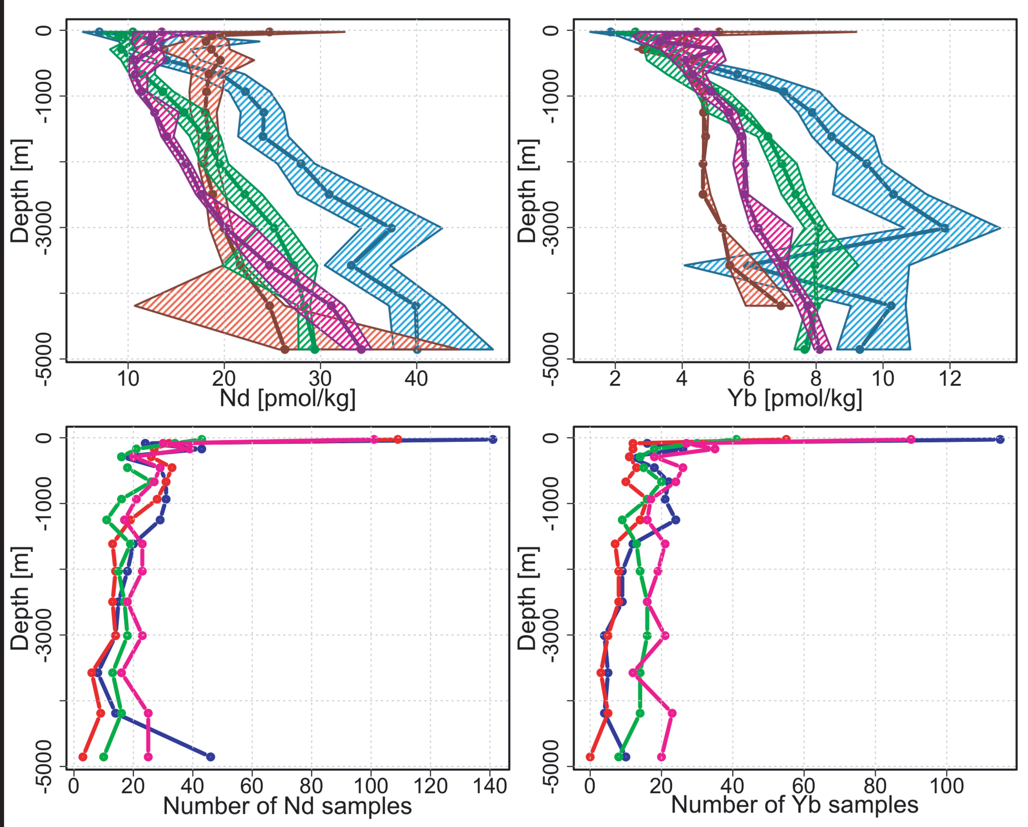

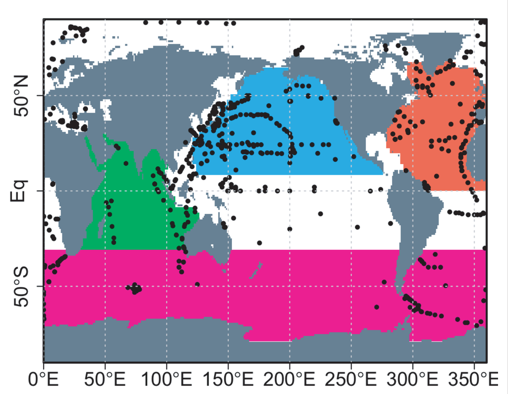

Figure 1: Typical vertical profiles of a) **Nd** and b) **Yb** for the regions shown on the map (c). Shading contains the 25th and 75th percentiles of the available data at each depth. Lines show the median. d,e) Vertical profiles of the number of samples available in the respective regions.

If you would like to (or could be convinced to) contribute data to add to this dataset, please contact us.

Thanks to Catherine Jeandel, Melanie Grenier, Ester Garcia Solson, for their willingness to share unpublished data.

Methodology

Numerical simulations are performed using the **Transport Matrix** formalism of Khatiwala (2005, 2007) (2.8°x2.8° forward MITgcm). This is used in conjunction with explicit estimates of boundary fluxes for rivers and dust intially developed for Nd (Jeandel et al. 2007). River and dust fluxes for the other REE are obtained by scaling the Nd boundary fluxes with shale concentration or measured river patterns.

Four **particle types** are considered for scavenging: particulate organic matter (**POM**), **$CaCO_3$**, **opal** and **dust**. The **reversible scavenging model** of Bacon and Anderson (1982) is used to separate dissolved and particulate components. Surface fluxes for POM, $CaCO_3$ and opal are from Henson et al. (2012). Surface dust flux estimates are from Mahowald et al. (2005). Typical remineralization profiles with length-scales specific to POM, $CaCO_3$ and opal are used to infer the interior particle field (Figure 2). The dust flux is assumed constant with depth.

Only a fraction (BF=**Bottom Flux**) of the particle flux reaching the seafloor is allowed to sediment out of the system. The fraction (1-BF) is forced to redissolve in the bottom-most cells of the model.

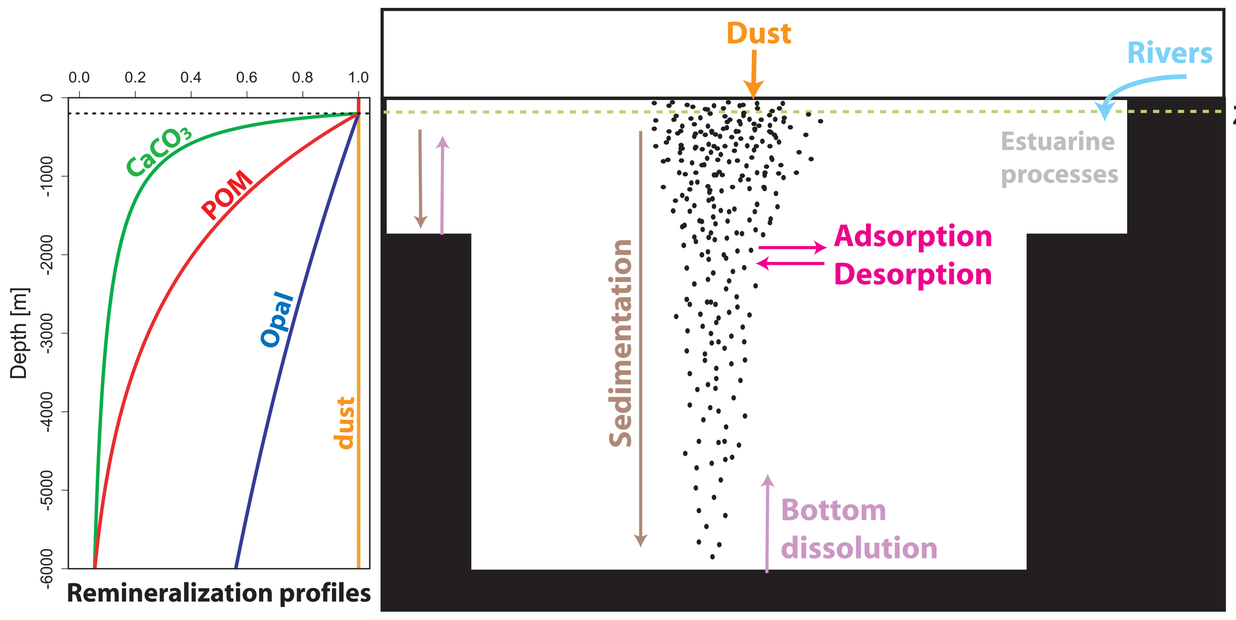

Figure 2: Main processes captured by the model and basic shapes of the remineralization profiles used to simulate particle mass at depth. Note the similarity between dust and opal profiles and between POM and $CaCO_3$ profiles. Because continental margins are shallower, the particle flux reaching the bottom above them is also large, resulting in a burial and strong bottom dissolution flux there (BF is assumed spatially constant here).

"Best-fit" estimates of the equilibrium scavenging coefficients

Inverse estimates of the equilibrium scavenging constants (K_d) were calculated for the case BF=0.1. Optimization was achieved by minimizing the sum of square error calculated between the observations and the model estimates subsampled at the same locations (see Figure 1c-e). The spatial distribution of available samples vary from REE to REE. Performance tests using **error-free synthetic data sets** (generated by subsampling foward model runs) instead of the observations and random initial guesses showed that the inversion results were **replicable** and systematically **converged** towards the correct parameter values.

The best-fit estimates of the K_d-values resulting from fitting the model to the available data using 50 random sets of initial guesses show **substantial scatter.** Scatter around estimates of K_{car} and K_{opal} is negligible for Nd, however, which is the REE with the most samples. Limiting the results to values of $\log_{10}(K_{car})>4.7$ and $\log_{10}(K_{opal})>6$, as indicated by the Nd results, one can (see Figure 3):

1) recover K_d-values for each particle type that are **in general agreement with published estimates**,
2) recover **systematic patterns** of the K_d-values for carbonates and opal particles,
3) confirm the results of Siddall et al. (2008), who suggested that **K_{POM} is small**. $\log_{10}(K_{POM})$ is likely smaller than 2-3 (expected from Balistrieri et al. (1981), Byrne and Kim (1990))

The fact that the magnitude and the range (from LREE to HREE) of the $\log_{10}(K_{opal})$ values are greater than the $\log_{10}(K_{car})$ values (and any other K-values) suggests that scavenging over the **Southern Ocean** exerts a global control on the REE distribution elsewhere. This association with the Southern Ocean is also consistent with the fact that REE concentrations are strongly correlated with Si concentrations.

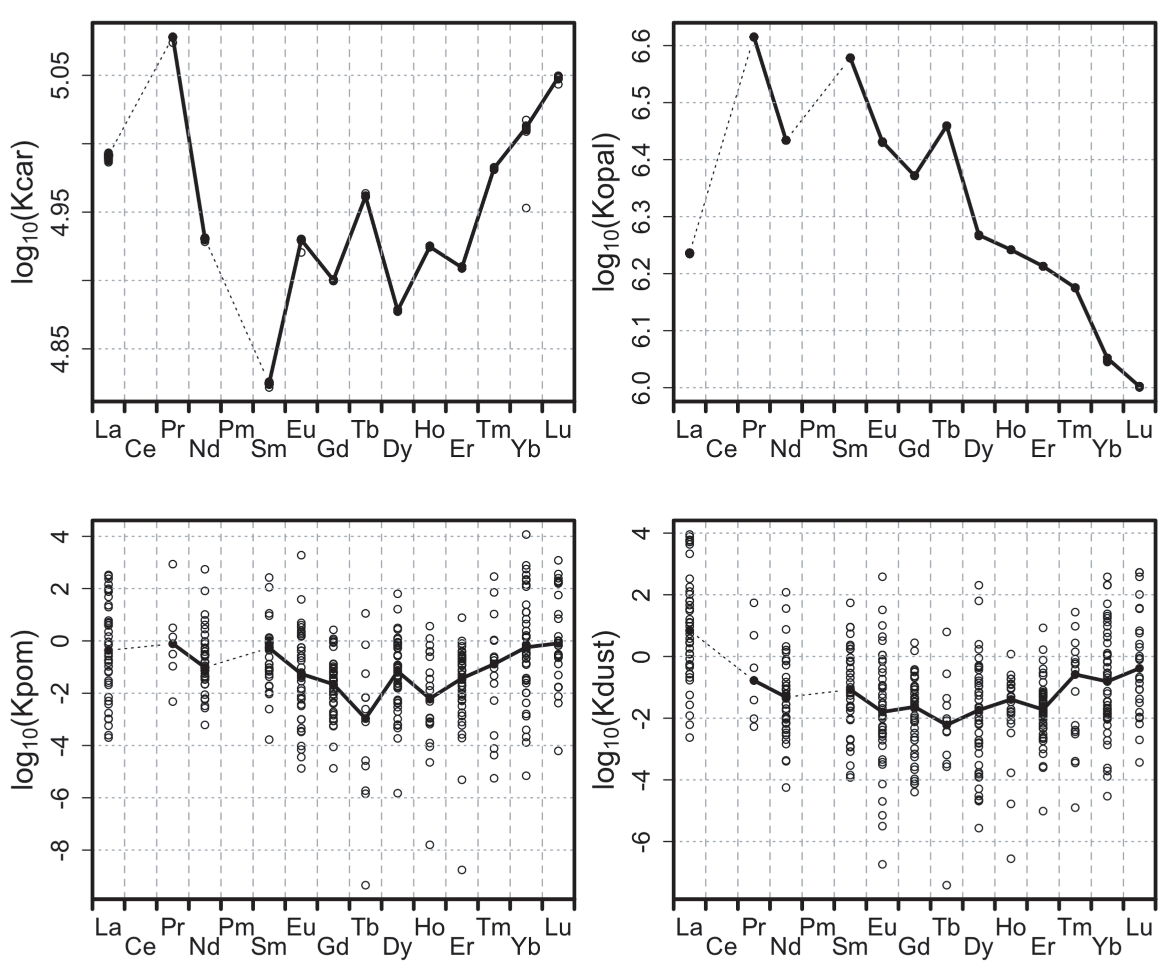

Figure 3: REE patterns of the log10(Kd) values for each particle type (carbonate, opal, organic matter and lithogenics). The line across the pattern links the median values of the trials shown in each panel.

For comparison, for Nd:

Sidall et al. (2008):
$\log_{10}(K_{car})=5.3$, $\log_{10}(K_{opal})=5.78$, $\log_{10}(K_{dust})=6.46$, $\log_{10}(K_{POM})=0$.

Arsouze et al. (2009),:
$\log_{10}(K_{car})=5.20$, $\log_{10}(K_{opal})=4.56$, $\log_{10}(K_{dust})=5.66$, $\log_{10}(K_{POM,small})=7.15$ and $\log_{10}(K_{POM,large})=4.72$.

Rempfer et al. (2011):
$\log_{10}(K_{car})=5.97$, $\log_{10}(K_{opal})=5.49$, $\log_{10}(K_{dust})=5.90$, $\log_{10}(K_{POM})=5.65$

Sensitivity analyses

The low computational cost of the Matrix method allows for many **parameter sensitivity experiments**. Experiments were performed that systematically vary the equlibrium partition coefficients of each particle type, the bottom flux fraction and the strengths of the dust and river sources and the particle fluxes themselves. Results hightlight the importance of regional controls (Southern Ocean, margins) and processes (sedimentary dissolution) (see Figures 4 and 5). Somes examples are shown here.

Figure 4: Modulating the dust source has a stronger influence on the absolute concentrations than changing the river flux by the same factor in the current model setup (caveat: Initial source ratio is 1.26 so inflation factor for dust has more influence).

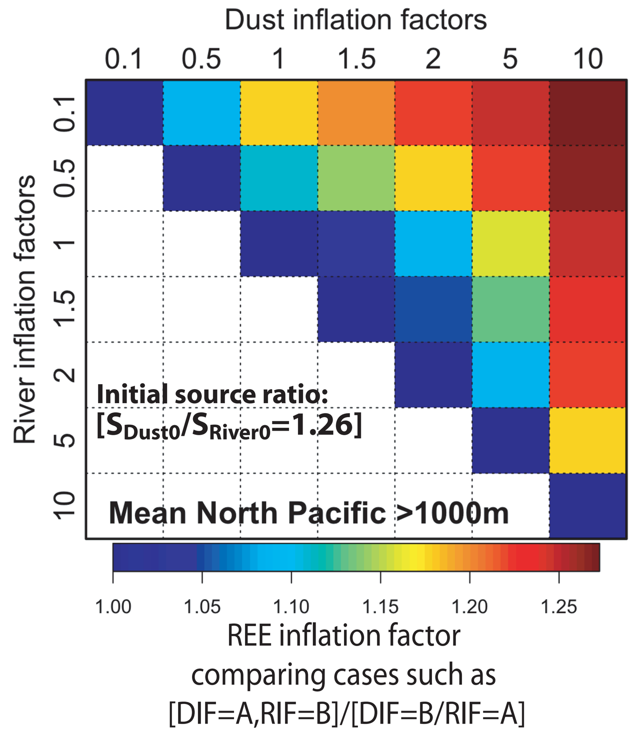

A significant amount of the river flux is lost by estuarine processes. Also, most of the river discharge occurs over margins, where particle fluxes and sedimentation are strongest.

When both dust and river sources are modulated by the same amount, the REE response is linear (i.e. doubling both sources results in a doubling of the concentrations). **Changing source strength affects absolute concentrations but impact on horizontal and vertical gradients is small relative to effect of scavenging factors.**

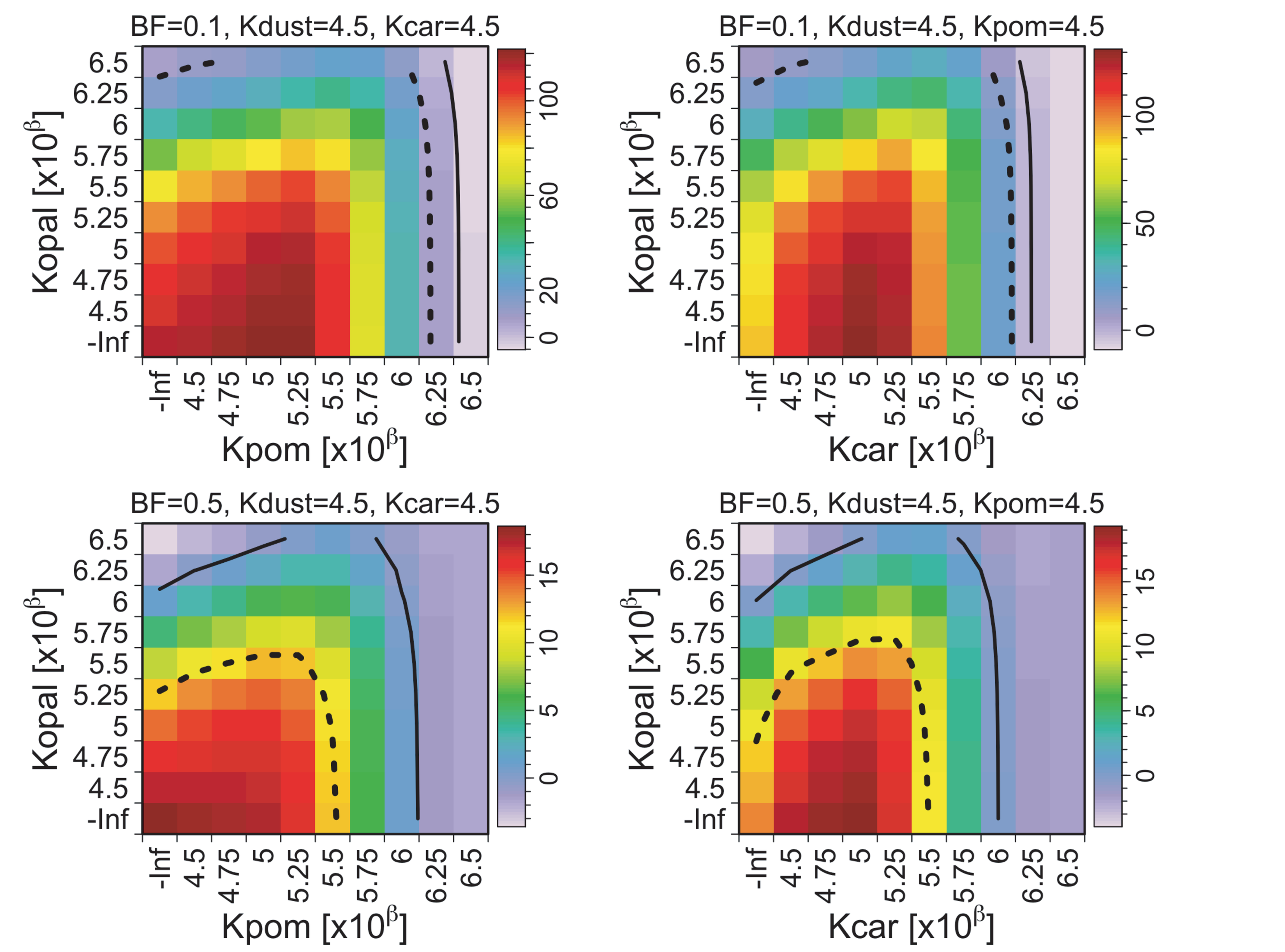

Figure 5: Evolution of the deep North Pacific to North Atlantic Nd-gradient as a function of equilibrium scavenging coefficients and for two scenario for the fate of the bottom sinking flux : (top row) BF=0.1 (90% redissolution) and (bottom row) BF=0.5 (50% redissolution). Dashed contours = observed NPAC-NATL Nd gradient.; solid contours = 0; negative values are inconsistent with observations.

Conclusions and outlooks

1) Equilibrium **scavenging constants for opal are greater** than for any other particle type.

2) The equilibrium **scavenging constant for organic matter is relatively small**, in accord with chemical considerations (e.g. Balistrieri et al. 1981, Byrne and Kim 1990) but in contrast with values obtained in other Nd-modeling studies.

3) Importance of opal scavening points towards the **Southern Ocean and margins** as location of particularly important locations for REE cycling. Role of particle dynamics will need to be addressed.

4) Sources and sinks are not well constrained but the main oceanic REE gradients are **controlled primarily by internal cycling processes**, in agreement with Oka et al. (2009). The model should include the possibility that K-values respond to their environment (e.g. pH, complexation, etc.).

5) The fate of the particles reaching the seafloor can have a substantial influence on the model results. Better parameterizations for the **sedimentary redissolution flux** are necessary.

6) Limited data coverage in the ocean and lack of **measured dissolved-particulate distribution coefficients** for different particle types limits understanding or REE (and generally metal) cycling.

References

Arsouze et al. (2009). Biogeosciences, 6:2829-2846. -- **Bacon and Anderson (1982)**. JGR, 87(C3):2045-2056. -- **Balistrieri et al. (1981)**. DSR 28A:101-121. -- **Byrne and Kim (1990)**. GCA, 54:2645-2656 -- **Byrne and Sholkovitz (1996)** Handbook on the Physics and chemistry of rare earth, 23, Ch158:497-593. -- **Chase et al. (2002)**. EPSL, 204:215-229. -- **Henson et al. (2012)**. GBC, GB1028. -- **Jeandel et al. (2007)**. Chem. Geol. 239:156-164. -- **Kato et al. (2011)**. Nature Geosciences, 4:535-539. -- **Khatiwala et al. (2005)**. Ocean modelling, 9:51-69. -- **Khatiwala (2007)**. GBC, GB3001. -- **Mahowald et al. (2005)**. GBC, 19(GB4025) -- **Oka et al. (2009)**. GBC, 23, GB4025. -- **Rempfer et al. (2011)**. GCA, 75:5927-5950. -- **Siddall et al. (2008)**. EPSL, 274:448-461.